Biochemical Journal (2019) **476** 3401–3411
https://doi.org/10.1042/BCJ20190687

Research Article

Allosteric changes in HDM2 by the ATM phosphomimetic S395D mutation: implications on HDM2 function

Lukas Uhrik[1,*], Lixiao Wang[2,*], Lucia Haronikova[1], Ixaura Medina-Medina[3], Yolanda Rebolloso-Gomez[3], Sa Chen[2], Borivoj Vojtesek[1], Robin Fahraeus[1,2,4], Lenka Hernychova[1] and Vanesa Olivares-Illana[3]

[1]Regional Centre for Applied Molecular Oncology, Masaryk Memorial Cancer Institute, Zluty Kopec 7, 656 53 Brno, Czech Republic; [2]Department of Medical Biosciences, Umeå University, SE-90185 Umeå, Sweden; [3]Laboratorio de Interacciones Biomoleculares y Cáncer, Instituto de Física Universidad Autónoma de San Luis Potosí, Zona Universitaria, Manuel Nava 6, 78290 San Luis Potosí, México; [4]Équipe Labellisée Ligue Contre le Cancer, INSERM UMR 1162, Université Paris 7, 27 Rue Juliette Dodu, 75010 Paris, France

Correspondence: Lenka Hernychova (lenka.hernychova@mou.cz) or Vanesa Olivares-Illana (vanesa@ifisica.uaslp.mx)

Allosteric changes imposed by post-translational modifications regulate and differentiate the functions of proteins with intrinsic disorder regions. HDM2 is a hub protein with a large interactome and with different cellular functions. It is best known for its regulation of the p53 tumour suppressor. Under normal cellular conditions, HDM2 ubiquitinates and degrades p53 by the 26S proteasome but after DNA damage, HDM2 switches from a negative to a positive regulator of p53 by binding to *p53* mRNA to promote translation of the *p53* mRNA. This change in activity is governed by the ataxia telangiectasia mutated kinase via phosphorylation on serine 395 and is mimicked by the S395D phosphomimetic mutant. Here we have used different approaches to show that this event is accompanied by a specific change in the HDM2 structure that affects the HDM2 interactome, such as the N-termini HDM2–p53 protein–protein interaction. These data will give a better understanding of how HDM2 switches from a negative to a positive regulator of p53 and gain new insights into the control of the HDM2 structure and its interactome under different cellular conditions and help identify interphases as potential targets for new drug developments.

Introduction

Intrinsically disordered regions (IDRs) in multi-domain proteins provide large flexibility into the molecule, contributing in this way to include in the same primary sequence, a variety of functions. This is one of the manners that evolution has optimised the genome functionality and diversity. Different conformations are affected allosterically via post-translational modifications, mutations or by the interaction with proteins or other macromolecules like DNA/RNA [1–6]. One example of this concept is the human proto-oncoprotein HDM2 (MDM2 in mouse). HDM2 is a hub in a complex network of interactions, with more than 100 interacting partners [7]. The focus of HDM2 studies has been on its central role in controlling the levels and activity of the p53 tumour suppressor. Mouse models have shown that the MDM2-null mouse develops early embryonic lethality that can be rescued by additional p53 deficiency [8]. HDM2 down-regulates the activity of p53 by acting as an E3 ubiquitin ligase of p53, promoting p53 proteasomal degradation [9,10] or by masking its transactivation domain [11] to control the nuclear export of p53 [12].

The ATM kinase (ataxia telangiectasia mutated kinase) is activated during DNA damage and is a key factor in p53 activation by direct or indirect phosphorylation of p53 N-terminal residues Ser15 and 20 (S15 and S20) [13,14]. However, mouse models show that these events are not sufficient for full activation of the p53-dependent DNA damage response [15–17]. Interestingly, HDM2 is also phosphorylated by ATM after DNA damage [18] on Ser395 (394 in mouse MDM2), which enables

*These authors contributed equally.

Received: 18 September 2019
Revised: 17 October 2019
Accepted: 21 October 2019

Accepted Manuscript online: 21 October 2019
Version of Record published: 15 November 2019

Biochemical Journal (2019) **476** 3401–3411
https://doi.org/10.1042/BCJ20190687

p53 stabilisation [19]. The importance of this phosphorylation site is underlined by the MDM2 S394A mice which displayed a defect in p53 activation [20]. The phosphorylation of HDM2 Ser395 is mimicked by the phosphomimetic mutant S395D and results in the binding of the C-terminal RING domain to the *p53* mRNA and an enhanced p53 translation [21–23]. The HDM2–*p53* mRNA interaction controls the E3 ubiquitin ligase substrate specificity and selectively prevents ubiquitination of p53 while not affecting ubiquitination of itself or of its homologue HDMX [23].

Examples of how post-translational modifications or the binding of macromolecules in multi-domain proteins induce allosteric changes have been reported. For example, the CK2 phosphorylation in Ser392 stabilises the tetramerisation domain of p53, promoting its oligomerisation [24]. The phosphomimetic mutant S392E yields a more thermostable protein with a change in conformation [25,26]. More recently, it has been shown by Raman spectroscopy how mutations in the p53 protein change its conformation [27]. An example of how small molecules induce allosteric changes in HDM2 was shown by Wallace et al. in 2006, who showed that a short peptides of the p53 box I domain, or the small molecule nutlin, provoked a conformational change that promoted a new interphase between MDM2's acidic domain and the p53 core domain [28]. It has also been reported that the phosphomimetic mutation S17D in the lid of MDM2 yields a more thermostable domain [25] and provokes an allosteric change that stimulates the interaction between the acidic domain and the DNA-binding domain of p53 [26].

In the present work, we used hydrogen–deuterium exchange mass spectrometry (HDX MS), limited proteolysis *in vitro* ubiquitination assay and protein modelling to demonstrate the impact of the phosphorylation site Ser395 on HDM2 structure and the functional repercussion on its E3 ubiquitin ligase activity. Here we show that HDM2 can adopt different conformations induced by post-translational modifications regulating in this way, the function of the protein. By dissecting these conformations, we can propose new interfaces for drug development that specifically target HDM2 activities during different cellular conditions.

Material and methods

Hydrogen–deuterium exchange mass spectrometry

Sample preparation: HDM2 proteins either wild type or mutant S395D (final concentration 1 μM in a sample loaded into LC–MS/MS) were diluted either with 50 mM of Tris–base and 150 mM of NaCl buffer in H_2O (pH 7.5) used for the preparation of the un-deuterated control and for the peptide mapping or with 50 mM of Tris–base and 150 mM of NaCl buffer in D_2O (pD 7.1) used for the preparation of the deuterated samples. The HDX was carried out at room temperature (RT) and was quenched at 10 and 45 min by the addition of 0.5 M of TCEP, 0.875 M of HCl in 1 M of glycine and 1 mg/ml of pepsin at a ratio of 10:3:5 (v/v/v), followed with 3 min of incubation at RT and rapid freezing in liquid nitrogen.

Digestion and HPLC separation: Each sample was thawed and injected into an LC-system (UltiMate 3000 RSLCnano, Thermo Scientific Dionex, Massachusetts, USA) to an immobilised nepenthesin enzymatic column (15 μl bed volume, flow rate of 20 μl/min, 2% acetonitrile/0.05% trifluoroacetic acid). Peptides were trapped and desalted on-line on a peptide microtrap (Michrom Bioresources, Auburn, CA, U.S.A.) for 3 min at a flow rate of 20 μl/min. Next, the peptides were eluted onto an analytical column (Jupiter C18, 1.0 × 50 mm, 5 μm, 300 Å, Phenomenex, CA, U.S.A.) and separated using a 2 min linear gradient elution of 10–40% B buffer in A buffer, followed by 31 min isocratic elution at 40% B. The solvents used were: buffer A — 0.1% formic acid in water and buffer B — 80% acetonitrile/0.08% formic acid. The immobilised nepenthesin column, trap cartridge and the analytical column were kept at 1°C.

Mass spectrometry and data analysis: Mass spectrometric analysis was carried out using an Orbitrap Elite mass spectrometer (Thermo Fisher Scientific, Massachusetts, USA) with ESI ionisation on-line connected with a robotic system based on the HTS-XT platform (CTC Analytics, Zwingen, Switzerland). The instrument was operated in a data-dependent mode for peptide mapping (HPLC–MS/MS). Each MS scan was followed by MS/MS scans of the top three most intensive ions from both the CID and HCD fragmentation spectra. Tandem mass spectra were searched using SequestHT against the cRap protein database (ftp://ftp.thegpm.org/fasta/cRAP), containing the sequence of both HDM2 proteins (wild type and mutant HDM2-S395D) with the following search settings: mass tolerance for precursor ions of 10 ppm, mass tolerance for fragment ions of 0.6 Da, no enzyme specificity, two maximum missed cleavage sites and no-fixed or variable modifications were applied. The false discovery rate at the peptide identification level was set at 1%. The sequence coverage was analysed with the Proteome Discoverer software version 1.4 (Thermo Fisher Scientific, Massachusetts, USA) and was

graphically visualised with MS Tools application (http://ms.biomed.cas.cz/MSTools/) [29]. Analysis of the deuterated samples was done in the LC–MS mode with ion detection in the orbital ion trap. The MS raw files together with the list of peptides (peptide pool) identified with high confidence characterised by the requested parameters (amino acid sequence of each peptide, its retention time, XCorr and ion charge) were processed using HDExaminer version 2.2 (Sierra Analytics, Modesto, CA, U.S.A.). The software analysed the peptides behaviour and created the uptake plots that showed peptide deuteration over time with a calculated confidence level (high and medium confidence is accepted, low confidence is rejected). The results from the peptide pool were displayed as a graph showing the evolution of deuteration at individual parts of the protein at the same time, and different protein states plotted using the GraphPad Prism version 5.03 for Windows (GraphPad Software, San Diego, CA, U.S.A.).

Purification of recombinant protein

Histidine-tagged recombinant proteins, HDM2, HDM2-S395D, HDM2(322–491) and HDM2(322–491)-S395D, were produced in *E. coli* BL21 (DE3) cells cultured at 37°C and purified using HiTrap nickel columns (GE Healthcare, Chicago, IL, USA). Lysis and buffer A (50 mM of Tris–base 200 mM of NaCl, 40 mM of imidazole, 10 μM of $ZnSO_4$, 10% of glycerol and were complemented with 10 mg of phenylmethanesulfonyl fluoride (PMSF, Sigma, Merck, Darmstadt, Germany). The pellet was resuspended in 10 ml of urea buffer (8 M urea, 50 mM of Tris–base, 150 mM of NaCl, 10 mM of imidazole, pH 8.5) and incubated for 2 h at RT. After centrifugation, the supernatant was loaded into the nickel column and washed with the following buffers; 25 ml of urea buffer, 25 ml of urea buffer plus 0.2% Triton, 25 ml of buffer A plus 10 mM of β-mercaptoethanol. Recombinant proteins were eluted from nickel columns with buffer B (50 mM of Tris–base, 200 mM of NaCl, 10 μM of $ZnSO_4$, 300 mM of imidazole, pH 8.5). Proteins were dialysed against phosphate buffer with 10 μM of $ZnSO_4$ and concentrated in centrifugal filter units Amicon (Merck Millipore, Darmstadt, Germany). Histidine-tagged recombinant p53 was induced at 15°C ON and purified on a HiTrap nickel column from the soluble fraction. Proteins were quantified and analysed in SDS–PAGE.

Limited proteolysis

Thirty micrograms of HDM2(322–491) and HDM2(322–491)-S395D were incubated with 0–100 ng of proteinase K (Thermo Fisher Scientific, Carlsbad, CA, USA) at 30°C for 2 or 5 min. The reaction was arrested by the addition of PMSF (final concentration 3 mM). The samples were analysed by SDS–PAGE.

In vitro ubiquitination assays

Ubiquitination reactions contained 25 mM of HEPES pH 8.0, 10 mM of $MgCl_2$, 4 mM of ATP, 0.5 mM of DTT, 0.05% (v/v) of Triton X-100, 0.25 mM of benzamidine, 10 mM of creatine phosphate, 3.5 units/ml of creatine kinase, ubiquitin or His-tagged ubiquitin (2 μg) and E1 (100 nM), E2 (1 μM) and p53 at 5 μg; the reactions were started with the addition of HDM2 or HDM2-S395D, incubated for 15 min at 30°C and analysed with 4–12% SDS–PAGE followed by immunoblotting with CM1 antibody (rabbit polyclonal sera to human p53 protein).

Results

Structural changes of HDM2 C-terminal domain due to phosphomimetic mutant S395D

It has been shown that during genotoxic stress, HDM2 is phosphorylated on Ser395, which switches the activity of HDM2 from an E3 ubiquitin ligase that acts as a negative regulator of p53 to an mRNA translation factor stimulating p53 synthesis [22,23]. To gain understanding into the structural mechanism behind the functional versatility of HDM2, we first studied the impact of the S395D phosphomimetic mutation on the C-terminal domain of (322–491) of HDM2 because this region comprises the site for *p53* mRNA binding but also contains the E3 ubiquitin ligase activity (Supplementary Figure S1).

We produced the recombinant C-terminal domain HDM2(322–491) wild type and HDM2(322–491)-S395D phosphomimetic mutant in *E. coli*. Using HDX MS, we studied the structural changes in the proteins imposed by the phosphomimetic mutation S395D. This is a powerful technique based on the solvent accessibility of the protein surface, measured as the replacement of the amide hydrogen by the deuterium atom on the amino acid [30,31]. The differences in the exchange reaction between the wild type and the phosphomimetic mutant

Biochemical Journal (2019) **476** 3401–3411
https://doi.org/10.1042/BCJ20190687

enable the study of the conformational flexibility. Firstly, the peptide mapping approach for both constructs was applied to create the library of peptides which covered the whole amino acid sequence. Either the wild type or the phosphomimetic mutant (final concentration of 1 μM) was diluted with a buffer in H_2O and used as a non-deuterated control. The samples were further processed by acidification and proteolytic digestion with pepsin and nepenthesin which was then measured using liquid chromatography connected with tandem MS (LC–MS/MS) to determine the amino acid sequences of created peptides under conditions used for HDX MS. We obtained 161 unique peptides of HDM2(322–491) wild type that covered 94% of its amino acid sequence in comparison with HDM2(322–491)-S395D when 171 unique peptides were identified with 100% of coverage (Supplementary Figure S2). The deuterium exchange of each construct (final concentration of 1 μM) was initiated by dilution with a buffer in D_2O carried out at RT. Deuteration was quenched at different point-times by the addition of quench buffer and then, rapid freezing in liquid nitrogen. After MS, the data were processed using *HDExaminer* software to evaluate changes in the deuteration of the peptides from HDM2(322–491) or HDM2(322–491)-S395D as a function of time. The data show a change in the profile of deuteration all along the protein construct and not just in the site of phosphorylation. HDM2(322–491) exhibited elevated HDX at 30 s and 10 min in comparison with HDM2(322–491)-S395D (Figure 1 and Supplementary Figure S3).

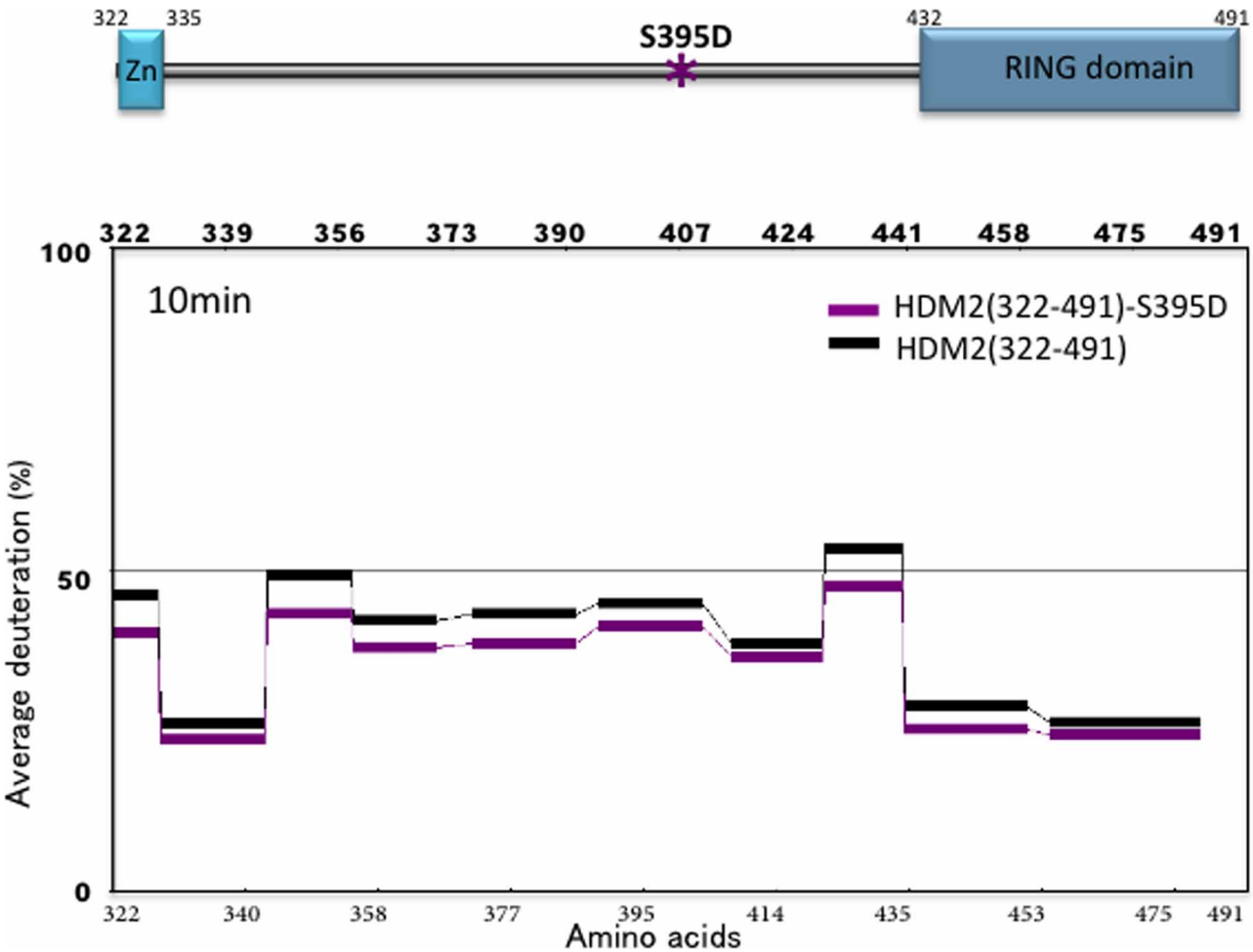

Figure 1. Hydrogen–deuterium exchange mass spectrometry of the C-terminal domain of HDM2 protein.

HDM2(322–491) wild type and HDM2(322–491)-S395D mutant difference in deuteration. In the upper panel, the schematic representation of the C-terminal construct of HDM2 is shown (Zn finger, RING the Ser395 is indicated with an asterisk). The data are plotted as % of deuteration of the peptide as a function of the numbering of the amino acids 321–491 after 10 min of incubation in the deuterated buffer. HDM2(322–491) (in black) and HDM2(322–491)-S395D (in purple). For other incubation times see Supplementary Figure S3A,B.

Biochemical Journal (2019) **476** 3401–3411
https://doi.org/10.1042/BCJ20190687

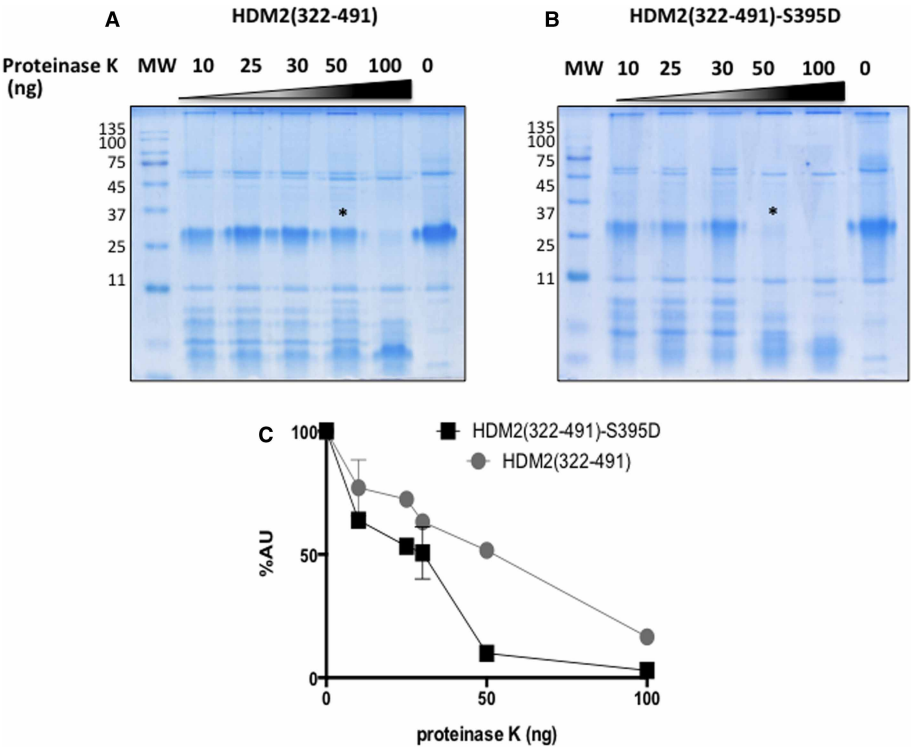

Figure 2. Limited proteolysis.

(**A**) HDM2(322–491) wild type and (**B**) the phosphomimetic mutant HDM2(322–491)-S395D by different concentrations of proteinase K. Asterisks represent the main differences between the wild type and the mutant. One representative experiment of three is shown. The incubation was performed with the different concentrations of proteinase K at 30°C for 2 min. (**C**) Quantification of the limited proteolysis showing that mutant HDM2(322–491)-S395D is more susceptible to proteinase K.

The conformational change in the structure of HDM2(322–491)-S395D was also observed using limited proteolysis by proteinases K [32]. The wild type and the phosphomimetic constructs were treated with concentrations ranging from 1 to 100 ng of proteinase K for 2 or 5 min at 30°C (Figure 2 and Supplementary Figure S4). The phosphomimetic mutant shows a higher susceptibility to proteolysis than the wild type construct, indicating a global change in the protein that exposes different cleavage sites. These results are in concordance with the HDX MS data that show a higher amount of unique peptides obtained with the phosphomimetic mutant after proteolytic digestion. Using the free modelling method QUARK [33,34], we built a model of the HDM2(322–491) and the phosphomimetic mutant HDM2(322–491)-S395D. The results revealed that this region of HDM2 has remarkable conformational plasticity and how this feature can be regulated by small changes such as post-translational modification. HDM2(322–491) shows a more globular structure where the RING domain (432–491 aa, in purple) is hidden in the core of the protein by the IDRs (322–431 aa). The Ser395 is in close proximity to the amino acids 464–471 in the α-helix of the RING domain and the model suggests that the phosphomimetic mutation opens the structure of the domain (Figure 3A,B). The surface exposed to the solvent increases almost three times from 419.18 $Å^2$ for the HDM2(322–491) until 1128.9 $Å^2$ for HDM2 (322–491)-S395D, indicating that different surfaces are exposed in the phosphomimetic mutant (Figure 3A,B, right panels). Together, these data help to explain how the phosphorylation on Ser395 alters HDM2 conformation results in the RING domain interacting with the *p53* mRNA during the DNA damage response.

Effect of phosphomimetic mutation in Ser395 on the HDM2 full-length structure

Multi-domain proteins often have IDRs that serve as a bridge between properly folded domains [35]. These IDRs are frequently the site of post-translational modifications that can regulate the conformation of the whole protein. To test this hypothesis, we produced full-length HDM2 and HDM2-S395D in a recombinant system

Biochemical Journal (2019) **476** 3401–3411
https://doi.org/10.1042/BCJ20190687

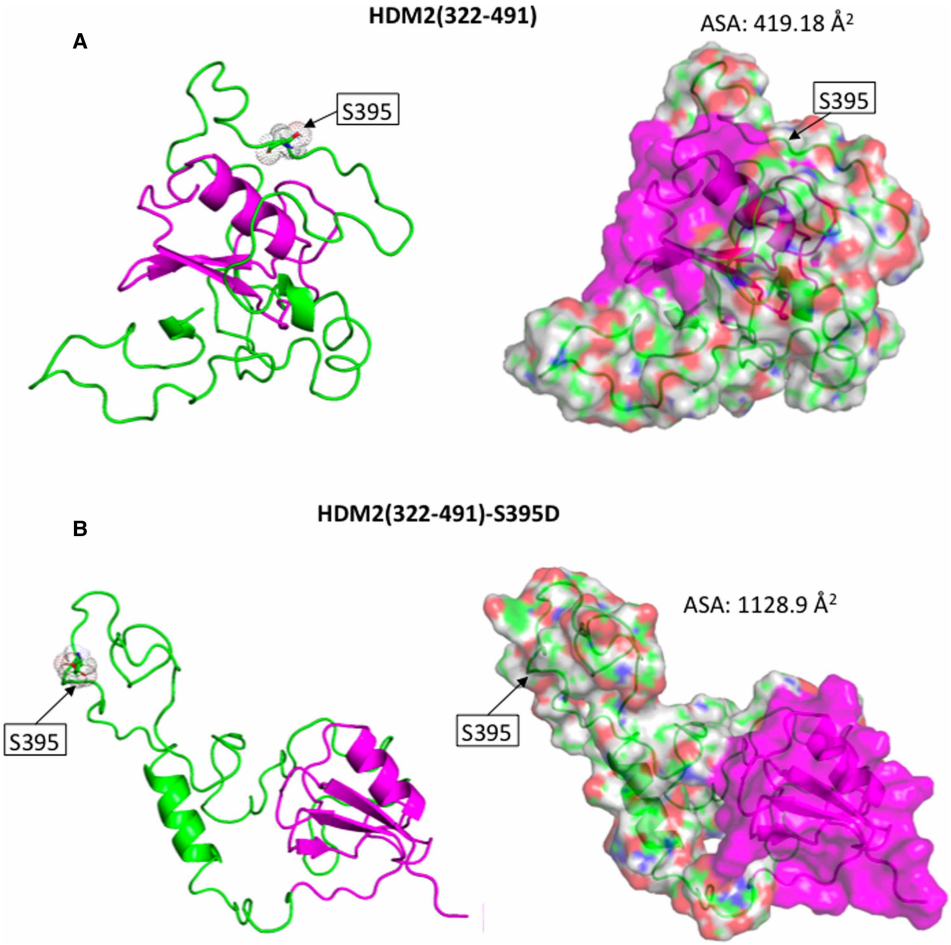

Figure 3. Molecular modelling of the C-terminal constructs of HDM2 wild type and phosphomimetic mutant.
The RING (432-491) domain is shown in purple and the position of Ser395 is highlighted. In the left panels, the cartoon models of the C-terminal constructs are shown and in the right panels, the surface representation of the two protein constructs is presented. (**A**) In the HDM2(322–491) wild type, the Ser395 is in close proximity to the RING domain. (**B**) In the HDM2(322–491)-S395D mutant, the structure is more open and the HDM2-S395D is distant from the RING domain. The models are presented using PyMOL [48,49].

and purified them (Supplemental Figure S5). The produced proteins were used in HDX MS to analyse the structural changes in the overall proteins due to the phosphomimetic mutation. Each protein at 1 μM was incubated in D_2O buffer under the same conditions as the C-terminal constructs. The results show that the small change in position 395 near to the RING domain in the C-terminus selectively disturbs two regions of the protein, without affecting the overall profile of the deuteration of the protein. The site next to the phosphorylation event occurs but also the hydrophobic pocket in the N-terminal part of the protein (1–100 aa) (Figure 4A,B and Supplementary Figure S6). The hydrophobic pocket of the HDM2 wild type was suppressed over time whilst part of the RING domain was more deuterated in comparison with HDM2-S395D. Additionally, the disorder tendency variations were performed with the HDM2 wild type and phosphomimetic mutant HDM2-S395D using PrDOS [36] which calculates the disorder probability of the protein. PrDOS characterises the disordered tendency of each amino acid along the protein sequence. The disorder probability can take a value between 0 and 1. The larger disorder probability, the higher disorder tendency of the amino acid is. Residues with a disorder probability above 0.5 are considered disordered, while residues with lower disorder probability considered to be ordered (Figure 4A,C). The data also show changes in the same two regions; the hydrophobic pocket and the Ser395 phosphorylation site near to the RING domain, confirming that there is no change in the overall structure, matching with the HDX MS results.

Biochemical Journal (2019) **476** 3401–3411
https://doi.org/10.1042/BCJ20190687

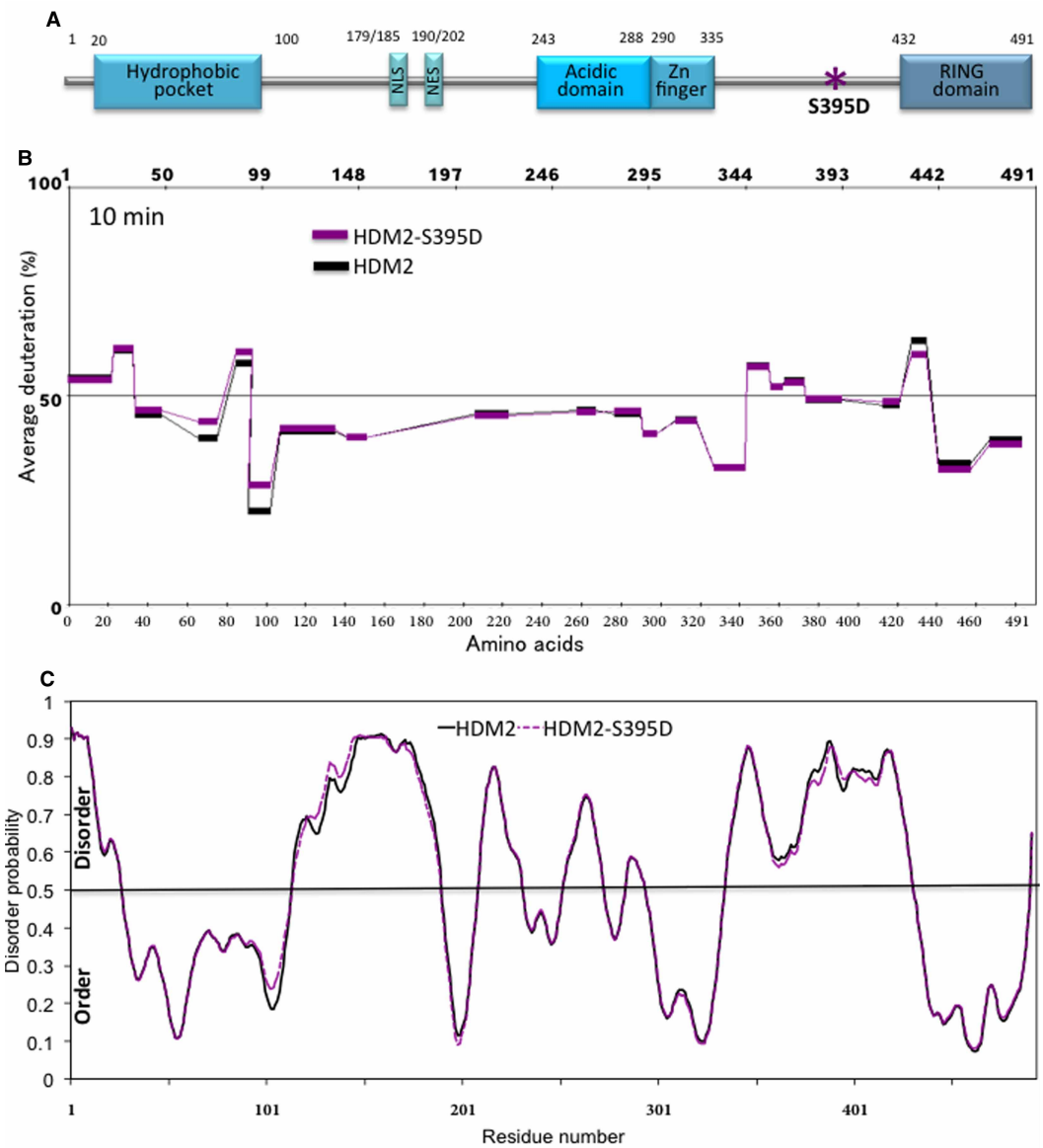

Figure 4. Effect of phosphomimetic mutation in Ser395 on the HDM2 full-length structure.

(**A**) Schematic representation illustrating the major domains of HDM2. NLS, nuclear localisation signal; NES, nuclear export signal; Zn, zinc finger; RING, really interesting new gene RING domain. (**B**) HDX MS of the full-length proteins HDM2 (in black) and HDM2-S395D (in purple). The data are plotted as % of deuteration of the peptide as a function of the numbering of the amino acids 1–491 after 10 min of incubation in the deuterated buffer. For other incubation times, see Supplementary Figure S6. (**C**) The predicted intrinsically disordered regions of HDM2 (in black) and HDM2-S395D (in purple).

Ubiquitination is altered by the phosphomimetic mutation

The functional implications of the phosphomimetic modification were observed by analysing the ubiquitination profile of p53. HDM2's capacity to interact and ubiquitinates p53 protein under normal cellular conditions has been well characterised *in vitro* [23,37,38]. It has been shown that the phosphorylation of Ser395 or the phosphomimetic S395D mutation has the same affinity towards p53 protein [23] and interestingly, that despite a similar affinity, it promotes the E3 ligase activity towards p53. It is only in the presence of the *p53* mRNA that HDM2 no longer is capable of ubiquitinating p53 while it retains the capacity to ubiquitinate its homologous protein HDMX and itself [23]. We compared the p53 ubiquitination profile by HDM2 wild type and HDM2-S395D. The data confirm that the HDM2-S395D phosphomimetic mutant is a better ubiquitin ligase

Biochemical Journal (2019) **476** 3401–3411
https://doi.org/10.1042/BCJ20190687

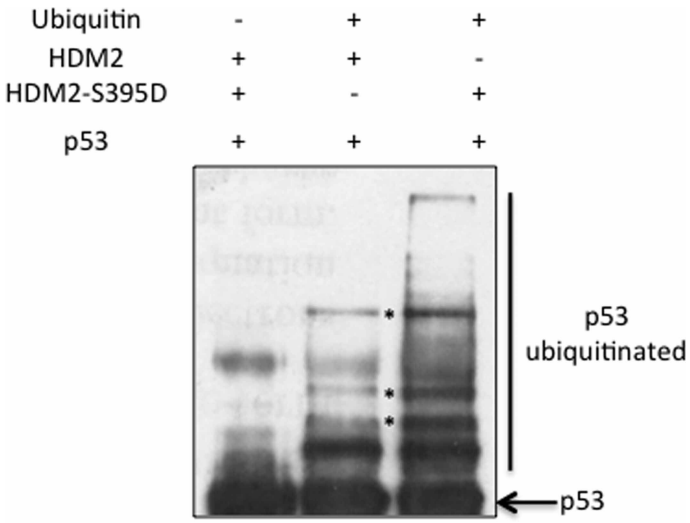

Figure 5. Ubiquitination of HDM2 and HDM2-S395D.

In vitro ubiquitination of recombinant p53 by HDM2 and HDM2-S395D. The first lane shows the control reaction without ubiquitin, the second lane shows p53 ubiquitination by the HDM2 wild type and the third lane shows the p53 ubiquitination by the HDM2-S395D mutant showing a higher ubiquitination profile. The asterisks show the increased bands of p53–ubiqutin complexes.

toward p53 and increases the amount of p53 ubiquitinated and the molecular mass of the p53–ubiquitin forms. This suggests that the plasticity of the protein and the domain organisation, rather than the affinity towards p53, are controlled by post-translational modifications and governs HDM2 E3 ligase activity towards p53, presumably by placing the E2 ligase in proximity to p53 lysine residues (Figure 5).

Discussion

The presented data support other studies showing that HDM2's interactions with its partner proteins are governed by a plasticity that is regulated by post-translation modification. Such events act together with protein–protein interactions to induce conformations that promote specific complex formations and HDM2-regulated functions. Besides, it is likely that allosteric change in one partner of such complex acts together with allosteric changes in the other and, thus, that inter allosteric changes take place between partners in the protein complexes in a reciprocal induced fit. For example, the HDM2 paralogous protein HDMX interacts with the N-terminal p53 binding domain and this first interaction promotes a secondary allosteric interaction between the p53 DNA-binding domain and the acidic domain of HDMX [39]. Similarly, ligands binding the hydrophobic N-terminal pocket like p53, p53-derived short peptides or small molecules promote allosteric changes in HDM2 that allow a secondary interaction between the acidic domain of HDM2 and the DNA-binding domain of p53 [28,40–42]. Additionally, another allosteric rearrangement has been reported involving the interaction of p53 in the N-terminal domain of HDM2 that enhances the HDM2 and HDMX interaction [38].

The deuteration profile of the C-terminal domain of HDM2 shows that the phosphomimetic mutant S395D promotes changes throughout the protein construct and exposes new surfaces. In comparison, the same mimetic change in the full-length HDM2 shows specific changes in two different domains. This likely reflects communication between the N- and C-terminal domains that together with the notion of interchangeable allosteric changes, emphasises that multi-domain proteins with intrinsically disordered domains are more than the sum of their parts (Supplementary Figure S7). The C-terminal constructs carrying the phosphomimetic mutant is more susceptible to limited proteolysis as compared with the wild type. However, Medina-Medina et al., in 2016, showed that the phosphomimetic full-length proteins instead protect HDM2 from proteolytic attacks [23]. This is in line with the idea that more N-terminal domains play a role in the structural rearrangement after phosphorylation. The *in silico* model of HDM2(322–491) in Figure 3 suggests that the phosphomimetic S395D results in the exposure of a larger surface to solvent and it is conceivable that this would also result in increased proteolysis. The peptide mapping of the C-terminal construct further supports the notion that the

phosphomimetic mutation opens the C-terminus. However, the HDX experiments show a decrease in the deuteration profile in the mutant (Figure 1). This could instead suggest that the protein is involved in another type of regulation. HDM2 has the ability to make oligomers and it is possible that the mutant opens up new surfaces of interaction that produce oligomers that can affect the degree of deuteration. One has to bear in mind that these are different assays and it illustrates the importance of a multi-assay approach and it will be interesting to see further structural studies to learn how to best interpret results using different assays.

HDM2 is overexpressed in ∼10% of human cancers, with large variations depending on cancer type, and acts as an oncoprotein when inactivating p53 [43–47]. However, under certain conditions such as ATM activation following DNA damage, HDM2 becomes a positive regulator of p53 protein [22]. The results presented here indicate that HDM2 following ATM-mediated phosphorylation on Ser395 is a better E3 ubiquitin ligase for p53 in the absence of *p53* mRNA. In a scenario when HDM2 is amplified and overexpressed in tumour cells, the constitutive activation of ATM due to genomic instability and the imbalance in the HDM2:*p53* mRNA ratio would result in no *p53* mRNA-bound HDM2 and an increase in p53 degradation and enhanced proliferation and tumour development.

HDM2 is considering as a good target for anti-cancer drug development programmes and several companies have developed drugs that bind the N-terminal hydrophobic pocket to prevent p53 interaction. However, this approach has been shown toxic in the clinic, which has resulted in a need to re-think how HDM2 can best be targeted to minimise the risk of undesirable effects. The results presented here highlight that cell condition-dependent interphases that are generated will help to identify compounds that more specifically target certain conformation of HDM2 and deliver more specific cell biological effects for personalised medicine.

Abbreviations

ATM kinase, ataxia telangiectasia mutated kinase; HDX, hydrogen–deuterium exchange; IDRs, intrinsically disordered regions; MS, mass spectrometry; PMSF, phenylmethanesulfonyl fluoride; RT, room temperature.

Author Contribution

L.U. and Lu.H. performed HDX MS experiments and analysed the data; Le.H. designed HDX MS experiments and analysed the data; L.W. performed the models and the IDR analysis; I.M.-M., S.C. and Y.R.-G. performed the experiments of proteolysis and ubiquitination and analysed the data; R.F. and B.V. supervised the project and analysed the data; V.O.-I. designed experiments, analysed the data and wrote the MS. All authors edited the MS.

Funding

This work was supported by Conacyt CB-256637 by projects MEYS — NPS I — LO1413 and MH CZ — DRO (MMCI, 00209805) and ECOS-Nord Program Cooperation Mexico-France No 249553. Cátedra Marcos Moshinsky 2017. B.V. was partially supported by the Grant Agency of the Czech Republic [Grant No. 19-03796S]. Cancerforskningsfonden Norr; Cancerfonden [180296] and Vetenskapsradet.

Competing Interests

The Authors declare that there are no competing interests associated with the manuscript.

References

1 Guo, J. and Zhou, H.X. (2016) Protein allostery and conformational dynamics. *Chem. Rev.* **116**, 6503–6515 https://doi.org/10.1021/acs.chemrev.5b00590
2 Rubin, S.M. (2013) Deciphering the retinoblastoma protein phosphorylation code. *Trends Biochem. Sci.* **38**, 12–19 https://doi.org/10.1016/j.tibs.2012.10.007
3 Akabas, M.H. (2015) Cysteine modification: probing channel structure, function and conformational change. *Adv. Exp. Med. Biol.* **869**, 25–54 https://doi.org/10.1007/978-1-4939-2845-3_3
4 Kitayner, M., Rozenberg, H., Kessler, N., Rabinovich, D., Shaulov, L., Haran, T.E. et al. (2006) Structural basis of DNA recognition by p53 tetramers. *Mol. Cell* **22**, 741–753 https://doi.org/10.1016/j.molcel.2006.05.015
5 Nussinov, R. and Tsai, C.J. (2015) Allostery without a conformational change? Revisiting the paradigm. *Curr. Opin. Struct. Biol.* **30**, 17–24 https://doi.org/10.1016/j.sbi.2014.11.005
6 Burch, L.R., Midgley, C.A., Currie, R.A., Lane, D.P. and Hupp, T.R. (2000) Mdm2 binding to a conformationally sensitive domain on p53 can be modulated by RNA. *FEBS Lett.* **472**, 93–98 https://doi.org/10.1016/S0014-5793(00)01427-7
7 Fahraeus, R. and Olivares-Illana, V. (2014) MDM2's social network. *Oncogene* **33**, 4365–4376 https://doi.org/10.1038/onc.2013.410

Biochemical Journal (2019) **476** 3401–3411
https://doi.org/10.1042/BCJ20190687

8 Jones, S.N., Roe, A.E., Donehower, L.A. and Bradley, A. (1995) Rescue of embryonic lethality in Mdm2-deficient mice by absence of p53. *Nature* **378**, 206–208 https://doi.org/10.1038/378206a0

9 Kubbutat, M.H., Jones, S.N. and Vousden, K.H. (1997) Regulation of p53 stability by Mdm2. *Nature* **387**, 299–303 https://doi.org/10.1038/387299a0

10 Honda, R., Tanaka, H. and Yasuda, H. (1997) Oncoprotein MDM2 is a ubiquitin ligase E3 for tumor suppressor p53. *FEBS Lett.* **420**, 25–27 https://doi.org/10.1016/S0014-5793(97)01480-4

11 Oliner, J.D., Pietenpol, J.A., Thiagalingam, S., Gyuris, J., Kinzler, K.W. and Vogelstein, B. (1993) Oncoprotein MDM2 conceals the activation domain of tumour suppressor p53. *Nature* **362**, 857–860 https://doi.org/10.1038/362857a0

12 Tao, W. and Levine, A.J. (1999) Nucleocytoplasmic shuttling of oncoprotein Hdm2 is required for Hdm2-mediated degradation of p53. *Proc. Natl Acad. Sci. U.S.A.* **96**, 3077–3080 https://doi.org/10.1073/pnas.96.6.3077

13 Dumaz, N. and Meek, D.W. (1999) Serine15 phosphorylation stimulates p53 transactivation but does not directly influence interaction with HDM2. *EMBO J.* **18**, 7002–7010 https://doi.org/10.1093/emboj/18.24.7002

14 Chehab, N.H., Malikzay, A., Stavridi, E.S. and Halazonetis, T.D. (1999) Phosphorylation of Ser-20 mediates stabilization of human p53 in response to DNA damage. *Proc. Natl Acad. Sci. U.S.A.* **96**, 13777–13782 https://doi.org/10.1073/pnas.96.24.13777

15 Chao, C., Hergenhahn, M., Kaeser, M.D., Wu, Z., Saito, S., Iggo, R. et al. (2003) Cell type- and promoter-specific roles of Ser18 phosphorylation in regulating p53 responses. *J. Biol. Chem.* **278**, 41028–41033 https://doi.org/10.1074/jbc.M306938200

16 Sluss, H.K., Armata, H., Gallant, J. and Jones, S.N. (2004) Phosphorylation of serine 18 regulates distinct p53 functions in mice. *Mol. Cell Biol.* **24**, 976–984 https://doi.org/10.1128/MCB.24.3.976-984.2004

17 Wu, Z., Earle, J., Saito, S., Anderson, C.W., Appella, E. and Xu, Y. (2002) Mutation of mouse p53 Ser23 and the response to DNA damage. *Mol. Cell Biol.* **22**, 2441–2449 https://doi.org/10.1128/MCB.22.8.2441-2449.2002

18 Khosravi, R., Maya, R., Gottlieb, T., Oren, M., Shiloh, Y. and Shkedy, D. (1999) Rapid ATM-dependent phosphorylation of MDM2 precedes p53 accumulation in response to DNA damage. *Proc. Natl Acad. Sci. U.S.A.* **96**, 14973–14977 https://doi.org/10.1073/pnas.96.26.14973

19 Maya, R., Balass, M., Kim, S.T., Shkedy, D., Leal, J.F., Shifman, O. et al. (2001) ATM-dependent phosphorylation of Mdm2 on serine 395: role in p53 activation by DNA damage. *Genes Dev.* **15**, 1067–1077 https://doi.org/10.1101/gad.886901

20 Gannon, H.S., Woda, B.A. and Jones, S.N. (2012) ATM phosphorylation of Mdm2 Ser394 regulates the amplitude and duration of the DNA damage response in mice. *Cancer Cell* **21**, 668–679 https://doi.org/10.1016/j.ccr.2012.04.011

21 Naski, N., Gajjar, M., Bourougaa, K., Malbert-Colas, L., Fahraeus, R. and Candeias, M.M. (2009) The p53 mRNA-Mdm2 interaction. *Cell Cycle* **8**, 31–34 https://doi.org/10.4161/cc.8.1.7326

22 Gajjar, M., Candeias, M.M., Malbert-Colas, L., Mazars, A., Fujita, J., Olivares-Illana, V. et al. (2012) The p53 mRNA-Mdm2 interaction controls Mdm2 nuclear trafficking and is required for p53 activation following DNA damage. *Cancer Cell* **21**, 25–35 https://doi.org/10.1016/j.ccr.2011.11.016

23 Medina-Medina, I., Garcia-Beltran, P., de la Mora-de la Mora, I., Oria-Hernandez, J., Millot, G., Fahraeus, R. et al. (2016) Allosteric interactions by p53 mRNA governs HDM2 E3 ubiquitin ligase specificity under different conditions. *Mol. Cell Biol.* **36**, 2195–2205 https://doi.org/10.1128/MCB.00113-16

24 Sakaguchi, K., Sakamoto, H., Lewis, M.S., Anderson, C.W., Erickson, J.W., Appella, E. et al. (1997) Phosphorylation of serine 392 stabilizes the tetramer formation of tumor suppressor protein p53. *Biochemistry* **36**, 10117–10124 https://doi.org/10.1021/bi970759w

25 Worrall, E.G., Worrall, L., Blackburn, E., Walkinshaw, M. and Hupp, T.R. (2010) The effects of phosphomimetic lid mutation on the thermostability of the N-terminal domain of MDM2. *J. Mol. Biol.* **398**, 414–428 https://doi.org/10.1016/j.jmb.2010.03.023

26 Fraser, J.A., Worrall, E.G., Lin, Y., Landre, V., Pettersson, S., Blackburn, E. et al. (2015) Phosphomimetic mutation of the N-terminal lid of MDM2 enhances the polyubiquitination of p53 through stimulation of E2-ubiquitin thioester hydrolysis. *J. Mol. Biol.* **427**, 1728–1747 https://doi.org/10.1016/j.jmb.2014.12.011

27 Hernández-Vidales, K., Guevara, E., Olivares-Illana, V. and González, F.J. (2019) Characterization of wild-type and mutant p53 protein by Raman spectroscopy and multivariate methods. *J. Raman Spectrosc.* **50**, 1388–1394 https://doi.org/10.1002/jrs.5655

28 Wallace, M., Worrall, E., Pettersson, S., Hupp, T.R. and Ball, K.L. (2006) Dual-site regulation of MDM2 E3-ubiquitin ligase activity. *Mol. Cell* **23**, 251–263 https://doi.org/10.1016/j.molcel.2006.05.029

29 Kavan, D. and Man, P. (2011) MSTools—web based application for visualization and presentation of HXMS data. *Int. J. Mass Spectrom.* **302**, 53–58 https://doi.org/10.1016/j.ijms.2010.07.030

30 Coufalova, D., Vojtesek, B. and Hernychova, L. [Utilization of hydrogen/deuterium exchange in biopharmaceutical industry]. *Klin. Onkol.* **29** (Suppl. 4), 59–63 https://doi.org/10.14735/amko20164S59

31 Klotz, I.M. and Frank, B.H. (1965) Deuterium–hydrogen exchange in amide N–H groups. *J. Am. Chem. Soc.* **87**, 2721–2728 https://doi.org/10.1021/ja01090a033

32 Reyes-Vivas, H., Martinez-Martinez, E., Mendoza-Hernandez, G., Lopez-Velazquez, G., Perez-Montfort, R., Tuena de Gomez-Puyou, M. et al. (2002) Susceptibility to proteolysis of triosephosphate isomerase from two pathogenic parasites: characterization of an enzyme with an intact and a nicked monomer. *Proteins* **48**, 580–590 https://doi.org/10.1002/prot.10179

33 Xu, D. and Zhang, Y. (2012) Ab initio protein structure assembly using continuous structure fragments and optimized knowledge-based force field. *Proteins* **80**, 1715–1735

34 Xu, D. and Zhang, Y. (2013) Toward optimal fragment generations for ab initio protein structure assembly. *Proteins* **81**, 229–239 https://doi.org/10.1002/prot.24179

35 Peng, Z., Mizianty, M.J. and Kurgan, L. (2014) Genome-scale prediction of proteins with long intrinsically disordered regions. *Proteins* **82**, 145–158 https://doi.org/10.1002/prot.24348

36 Ishida, T. and Kinoshita, K. (2007) PrDOS: prediction of disordered protein regions from amino acid sequence. *Nucleic Acids Res.* **35**, W460–W464 https://doi.org/10.1093/nar/gkm363

37 Momand, J., Zambetti, G.P., Olson, D.C., George, D. and Levine, A.J. (1992) The mdm-2 oncogene product forms a complex with the p53 protein and inhibits p53-mediated transactivation. *Cell* **69**, 1237–1245 https://doi.org/10.1016/0092-8674(92)90644-R

38 Medina-Medina, I., Martinez-Sanchez, M., Hernandez-Monge, J., Fahraeus, R., Muller, P. and Olivares-Illana, V. (2018) P53 promotes its own polyubiquitination by enhancing the HDM2 and HDMX interaction. *Protein Sci.* **27**, 976–986 https://doi.org/10.1002/pro.3405

39 Wei, X., Wu, S., Song, T., Chen, L., Gao, M., Borcherds, W. et al. (2016) Secondary interaction between MDMX and p53 core domain inhibits p53 DNA binding. *Proc. Natl Acad. Sci. U.S.A.* **113**, E2558–E2563 https://doi.org/10.1073/pnas.1603838113
40 Shimizu, H., Burch, L.R., Smith, A.J., Dornan, D., Wallace, M., Ball, K.L. et al. (2002) The conformationally flexible S9-S10 linker region in the core domain of p53 contains a novel MDM2 binding site whose mutation increases ubiquitination of p53 in vivo. *J. Biol. Chem.* **277**, 28446–28458 https://doi.org/10.1074/jbc.M202296200
41 Yu, G.W., Rudiger, S., Veprintsev, D., Freund, S., Fernandez-Fernandez, M.R. and Fersht, A.R. (2006) The central region of HDM2 provides a second binding site for p53. *Proc. Natl Acad. Sci. U.S.A.* **103**, 1227–1232 https://doi.org/10.1073/pnas.0510343103
42 Kawai, H., Wiederschain, D. and Yuan, Z.M. (2003) Critical contribution of the MDM2 acidic domain to p53 ubiquitination. *Mol. Cell Biol.* **23**, 4939–4947 https://doi.org/10.1128/MCB.23.14.4939-4947.2003
43 Toledo, F. and Wahl, G.M. (2007) MDM2 and MDM4: p53 regulators as targets in anticancer therapy. *Int. J. Biochem. Cell Biol.* **39**, 1476–1482 https://doi.org/10.1016/j.biocel.2007.03.022
44 Toledo, F. and Wahl, G.M. (2006) Regulating the p53 pathway: in vitro hypotheses, in vivo veritas. *Nat. Rev. Cancer* **6**, 909–923 https://doi.org/10.1038/nrc2012
45 Oliner, J.D., Saiki, A.Y. and Caenepeel, S. (2016) The role of MDM2 amplification and overexpression in tumorigenesis. *Cold Spring Harb. Perspect. Med.* **6** https://doi.org/10.1101/cshperspect.a026336
46 Coindre, J.M., Pedeutour, F. and Aurias, A. (2010) Well-differentiated and dedifferentiated liposarcomas. *Virchows Arch.* **456**, 167–179 https://doi.org/10.1007/s00428-009-0815-x
47 Momand, J., Jung, D., Wilczynski, S. and Niland, J. (1998) The MDM2 gene amplification database. *Nucleic Acids Res.* **26**, 3453–3459 https://doi.org/10.1093/nar/26.15.3453
48 DeLano, W.L. (2002) *PyMOL*, DeLano Scientific LLC, San Carlos, CA
49 DeLano, W.L. (2009) *The PyMOL Molecular Graphics System*, DeLano Scientific LLC, San Carlos, CA